Head and Neck Pathology (2023) 17:33–52
https://doi.org/10.1007/s12105-022-01518-6

SPECIAL ISSUE: TOP TEN HEAD AND NECK DIFFERENTIALS

Top 10 Clear Cell Head and Neck Lesions to Contemplate

Nicole A. Cipriani[1] · **Aanchal Kakkar**[2]

Received: 4 November 2022 / Accepted: 27 November 2022 / Published online: 16 March 2023

Abstract

Background Optically clear cytoplasm may occur in neoplastic and non-neoplastic conditions, either as a characteristic feature of a disease entity or as a morphologic rarity, potentially creating diagnostic dilemmas in various organ systems. In the head and neck, clear cell change can occur in lesions of salivary, odontogenic, thyroid, parathyroid, or sinonasal/skull base origin, as well as in metastases to these regions.

Methods This review elaborates the top ten clear cell lesions in the head and neck, emphasizing their distinguishing histologic, immunohistochemical, and molecular attributes, and presents a rational approach to arriving at an accurate classification.

Results Cytoplasmic pallor or clearing may be caused by accumulations of glycogen, lipid, mucin, mucopolysaccharides, water, foreign material, hydropic organelles, or immature zymogen granules. Overlapping morphologic features may present a diagnostic challenge to the surgical pathologist. Similarity in immunohistochemical profiles, often due to common cell type, as well as rare non-neoplastic mimics, furthers the diagnostic conundrum.

Conclusions The top ten lesions reviewed in this article are as follows: (1) clear cell carcinoma (salivary and odontogenic), (2) mucoepidermoid carcinoma, (3) myoepithelial and epithelial-myoepithelial carcinoma, (4) oncocytic salivary gland lesions, (5) squamous cell carcinoma, (6) parathyroid water clear cell adenoma, (7) metastatic renal cell carcinoma (especially in comparison to clear cell thyroid neoplasms), (8) sinonasal renal cell-like adenocarcinoma, (9) chordoma, and (10) rhinoscleroma.

Keywords Head and neck · Clear cell · Salivary · Thyroid · Odontogenic · Sinonasal · Skull base

Introduction

Optically clear cytoplasm may occur in neoplastic and non-neoplastic conditions, either as a characteristic feature of a disease entity or as a morphologic rarity, potentially creating diagnostic dilemmas in various organ systems. Cytoplasmic pallor or clearing may be caused by accumulations of glycogen, lipid, mucin, mucopolysaccharides, water, foreign material, hydropic organelles, or immature zymogen granules [1, 2]. In the head and neck, clear cell change can occur in lesions of salivary gland, odontogenic, thyroid gland, parathyroid gland, or sinonasal/skull base origin, as well as in metastases to these regions [1–6]. Overlapping morphologic features may present a diagnostic challenge to the surgical pathologist. Similarity in immunohistochemical profiles, often due to common cell type, as well as rare non-neoplastic mimics, furthers the diagnostic conundrum. This review elaborates the top ten clear cell lesions in the head and neck, emphasizing their distinguishing histologic, immunohistochemical, and molecular attributes, and presents a rational approach to arriving at an accurate diagnosis. These top ten lesions include (1) clear cell carcinoma (salivary gland and odontogenic), (2) mucoepidermoid carcinoma, (3) myoepithelial and epithelial-myoepithelial carcinoma, (4) oncocytic salivary gland lesions, (5) squamous cell carcinoma, (6) parathyroid water clear cell adenoma, (7) metastatic renal cell carcinoma (especially in comparison to clear cell thyroid neoplasms), (8) sinonasal renal cell-like adenocarcinoma, (9) chordoma, and (10) rhinoscleroma (Table 1 and Fig. 1).

✉ Nicole A. Cipriani
Nicole.Cipriani@uchospitals.edu

[1] Department of Pathology, The University of Chicago, 5841 S. Maryland Ave, MC 6101, Chicago, IL 60637, USA

[2] All India Institute of Medical Sciences, Department of Pathology, Ansari Nagar, New Delhi, India

Table 1 Immunohistochemical Panel for the Differential Diagnosis of Clear Cell Lesions of the Head and Neck

Diagnosis	CK	EMA, CEA	CK7	p63, p40	S100	SMA, GFAP, calponin	SOX10	TTF1	mPAX8	PTH	CAIX, CD10	Other markers / Molecular findings
Clear cell MEca	+	−	−/+	+	+	+	+	−	−	-	-	*PLAG1* rearr *EWSR1* rearr
Clear cell EMC	+	+ (ductal)	+ (ductal)	+ (abluminal)	+ (abluminal)	+ (abluminal)	+	−	−	-	-	*PLAG1* rearr *HMGA2* rearr *HRAS* Q61R
HCCC	+	+	±	+	−	−	−	−	−	-	-	HMWK *EWSR1::ATF1* *EWSR1::CREM*
Clear cell MEC	+	+	+	+	−	−	−	−	−	-	-	HMWK *CRTC1/3::MAML2*
PA with clear cells	+	−	+ (ductal)	+ (abluminal)	+ (abluminal)	+ (abluminal)	+	−	−	-	-	*PLAG1* rearr *HMGA2* rearr
Clear cell oncocytoma	+	−/+	±	+ (basal cells)	−	−	−	−	−	-	-	-
SCC with clear cells	+	+	-/+	+	−	−	−	−	−	-	-	HMWK UV signature
Clear cell thyroid neoplasms	+	−	+	−	−	−	−	+	+	-	-	TG
Metastatic RCC	+	−	−	−	−	−	−	−	+	-	+	RCC marker
Water clear cell parathyroid adenoma	+	−	+	−	−	−	−	−	−	+	-	GATA3, CMG
Sinonasal RCC-like adenocarcinoma	+	±	+	−	−	−	−	−	−	-	+	RCC marker negative
Chordoma	+	+ (EMA)	-	−	+	−	−	−	−	-	-	Brachyury; *INI1* loss*
Clear cell chondrosarcoma	−	−	−	−	+	−	−	−	−		-	-
Rhinoscleroma	−	−	−	−	−	−	−	−	−	-	-	CD68

*In poorly differentiated chordomas

MEca myoepithelial carcinoma, *EMC* epithelial-myoepithelial carcinoma, *HCCC* hyalinizing clear cell carcinoma, *MEC* mucoepidermoid carcinoma, *PA* pleomorphic adenoma, *SCC* squamous cell carcinoma, *RCC* renal cell carcinoma, *CK* keratin, *EMA* epithelial membrane antigen, *CEA* carcinoembryonic antigen, *SMA* smooth muscle actin, *GFAP* glial fibrillary acidic protein, *mPAX8* monoclonal PAX8, *PTH* parathyroid hormone, *IHC* immunohistochemical, *HMWK* high molecular weight keratin, *UV* ultraviolet, *TG* thyroglobulin, *CMG* chromogranin, *rear* rearrangement

Fig. 1 Differential diagnosis summary of head and neck clear cell lesions

Clear Cell Carcinoma (Salivary Gland and Odontogenic)

Introduction and Epidemiology

Hyalinizing clear cell carcinoma (HCCC) is a malignant infiltrative neoplasm composed of clear to eosinophilic cells in a variably hyalinized stroma. It occurs over a wide age range, in minor salivary gland locations such as soft palate, base of tongue, and floor of mouth, among others [7]. Clear cell odontogenic carcinoma (CCOC) is a morphologically similar neoplasm that occurs in the gnathic bones, with the mandible being involved three to four times more frequently than maxilla [8].

Histologic, Immunohistochemical, and Molecular Findings

Histologically, both are infiltrative neoplasms composed of nests, cords, and trabeculae of small cells with clear to pale eosinophilic cytoplasm and monotonous small round to wrinkled nuclei with inconspicuous nucleoli, infrequent

mitoses, and mild pleomorphism (Fig. 2) [7]. Often, the tumor is composed entirely of eosinophilic cells. Squamous differentiation, intracellular mucin, occasional ducts, pagetoid spread into the adjacent epithelium, pseudo-sebaceous cells, and intranuclear pseudoinclusions may be seen [7]. The stroma is densely hyalinized to fibrocellular, with hyalinization being more prominent at the center than at the periphery of the tumor. CCOC has three morphological subtypes: biphasic: the most common, consisting of a dual population of clear and eosinophilic cells; monophasic: only clear cells; and ameloblastic: columnar cells showing evidence of ameloblastic differentiation [8]. Peripheral palisading and basaloid cells are variably present. Despite the bland morphology of tumor cells, perineural invasion is frequent in both tumors.

HCCC and CCOC are immunopositive with both low and high molecular weight keratin (HMWK), CK19, CK7, epithelial membrane antigen (EMA), p63, and p40; myoepithelial markers including smooth muscle actin (SMA), S100 protein, and calponin are negative [9]. Tumor cells contain intracytoplasmic PAS-positive diastase sensitive glycogen, at least focally. Diffuse p16 positivity has been identified in HCCC, with potential for misdiagnosis as human papillomavirus (HPV)-associated squamous cell carcinoma (SCC); however, negative RNA in situ hybridization (ISH) for high-risk HPV confirms the absence of virus [10]. Both HCCC and CCOC show *EWSR1* gene rearrangements, most commonly *EWSR1*::*ATF1* and rarely *EWSR1*::*CREM* gene fusions, which aid in differentiating them from most other clear cell tumors [11–13].

Differential Diagnosis and Clinical Implications

Differential diagnosis of HCCC includes SCC, mucoepidermoid carcinoma (MEC), and myoepithelial carcinoma rich in clear cells, all of which are discussed in detail below.

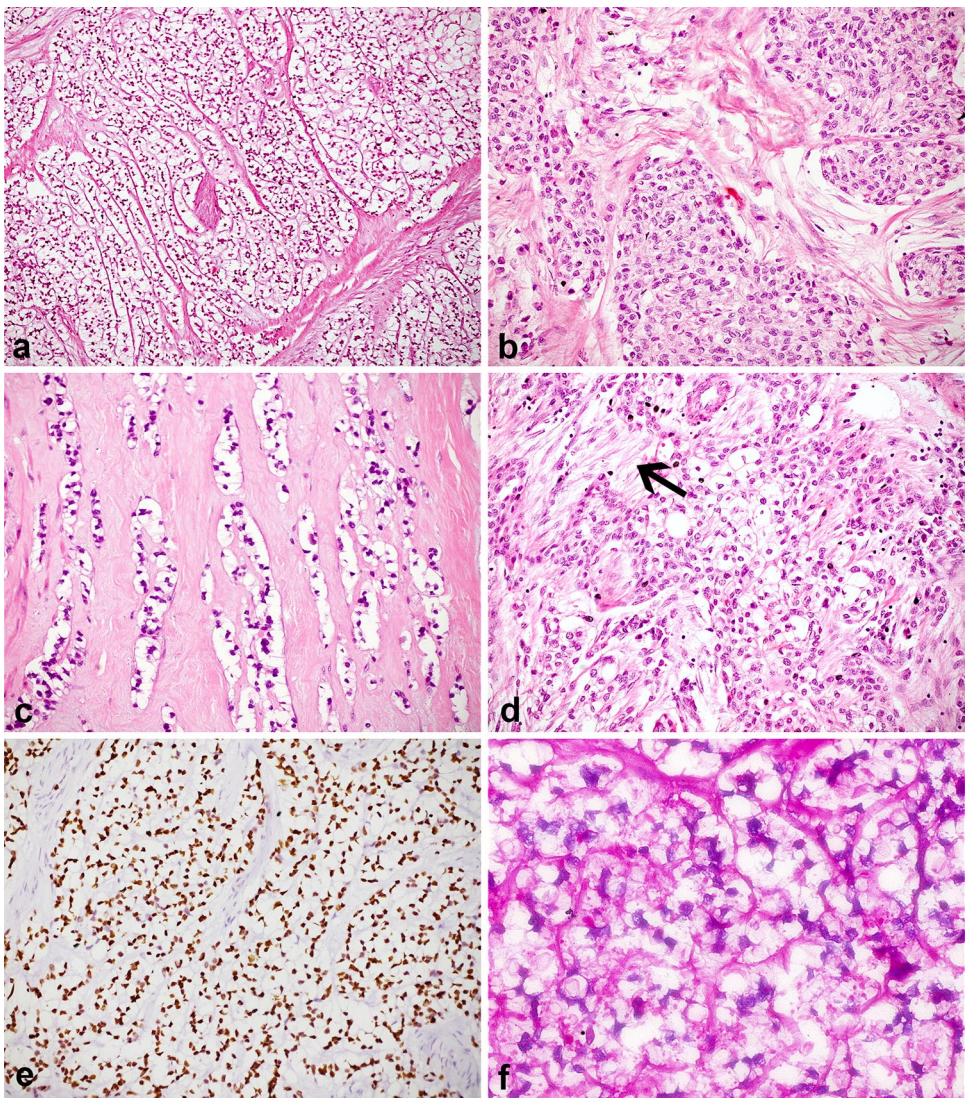

Fig. 2 Hyalinizing clear cell carcinoma is composed of cords of polygonal clear cells with small wrinkled nuclei (**a**). In areas, tumor cells have pale eosinophilic cytoplasm and are arranged in large nests (**b**). Stroma varies from hyalinized (**c**) to fibrocellular (**d**). Tumor cells are positive for p40 (**e**) and contain intracytoplasmic PAS-positive material (**f**)

HCCC lacks cystic spaces lined by mucous cells as seen in classic MEC, but the differential is more difficult in cases of clear cell MEC, which may lack cystic structures. Proving rearrangement of *EWSR1* (HCCC) versus *MAML2* (MEC) would be diagnostic. HCCC generally lacks the nuclear pleomorphism, frequent mitoses, and overlying epithelial dysplasia present in SCC. CCOC must be differentiated from clear cell calcifying epithelial odontogenic tumor (CEOT), odontogenic carcinoma with dentinoid (OCD), and metastatic carcinomas, particularly those with clear cells (i.e., renal cell carcinoma (RCC)). Clear cell CEOT would display foci of conventional CEOT, with polygonal epithelial cells with prominent intercellular bridges in sheets, amyloid-like material that stains positive with Congo Red, and calcifications [14]. OCD is a recently described tumor composed of cords and sheets of polygonal clear to squamoid cells with small vesicular nuclei; columnar cells with palisaded nuclei may be seen [15]. The presence of acellular eosinophilic dentinoid is the striking feature that facilitates its diagnosis, which is aided by immunopositivity for ß-catenin consequent to *CTNNB1* or *APC* mutations [16]. *EWSR1* rearrangements have not been described in clear cell CEOT or OCD.

Clear Cell Mucoepidermoid Carcinoma

Introduction and Epidemiology

MEC, the most common malignant salivary gland neoplasm, is an epithelial tumor composed of a varying proportion of squamoid/epidermoid, intermediate, and mucous cells arranged in solid-cystic patterns. However, several other cell types may be seen in MEC, including clear cells, oncocytic cells, ciliated columnar cells, and granular acinar cells. Although rare, MEC with a predominance of clear cells is referred to as clear cell MEC, and accounts for around 3% of all MEC [17]. It has been described in the buccal mucosa, palate, floor of mouth, and tongue, developing over a wide age range [18].

Histologic, Immunohistochemical, and Molecular Findings

Clear cell MECs display clear cells arranged in a nested pattern and may be devoid of cysts or glandular structures (Fig. 3). Cell borders are distinct; cytoplasm is abundant, optically clear and contains glycogen demonstrable on PAS staining with diastase digestion; nuclei are small to medium sized with conspicuous nucleoli [19]. Stromal hyalinization, when present, can lead to resemblance to HCCC. Epidermoid cells are rare to absent [20]. Tumor-associated lymphoid proliferation frequently present in conventional MEC has not been described in clear cell MEC [18, 19]; however, foci of calcification have been reported [21]. The neoplastic clear cells are immunopositive for squamous markers p63, p40, and CK5/6. If present, mucous cells would be positive for low molecular weight keratins, mucicarmine, and Alcian blue-PAS. They also retain PAS after diastase digestion. Currently, recommendations on grading of clear cell MEC do not exist, but when using the Brandwein system, these tumors would be at least intermediate grade due to the lack of an intracystic component [19, 22].

Differential Diagnosis and Clinical Implications

Differential diagnosis includes salivary clear cell carcinoma (CCC), primary and metastatic clear cell-rich squamous cell carcinoma (SCC), and myoepithelial cell neoplasms with prominent clear cells. Up to 80% of MEC harbor *CRTC1/3*::*MAML2* fusion genes, while CCC is characterized by *EWSR1*::*ATF1* fusion [20]. While clear cell MEC and clear myoepithelial cell-rich neoplasms both stain positively with squamous/basal markers p40 and p63, negativity for SOX10 and myoepithelial markers (i.e., SMA, calponin, glial fibrillary acidic protein (GFAP) and S100 protein) serves to distinguish clear cell MEC from clear myoepithelial cell-rich neoplasms [23]. Clear cell-rich SCC may show features of squamous differentiation such as keratinization and squamous pearls. As its immunohistochemical profile is identical to that of clear cell MEC, demonstration of *CRTC1/3*::*MAML2* rearrangement can confirm the diagnosis as clear cell MEC in challenging cases. These gene rearrangements can be demonstrated by FISH, RT-PCR, or next generation sequencing (NGS). While surrogate immunohistochemical markers are increasingly becoming available for diagnosis of salivary gland neoplasms that harbor characteristic gene rearrangements, the fusions in both MEC and CCC lack fusion proteins that are demonstrable by immunohistochemistry, thus necessitating molecular testing. Metastatic renal cell carcinoma (RCC) may also be considered in the differential diagnosis, as discussed below. Interestingly, focal CD10 positivity has been described in clear cell MEC and should be interpreted with caution, in conjunction with more specific immunohistochemical stains like PAX8, CAIX, and RCC antigen [18].

Clear Cell-Rich Myoepithelial Carcinoma and Epithelial-Myoepithelial Carcinoma

Introduction and Epidemiology

Myoepithelial carcinoma (MEca) is a rare invasive malignancy of salivary glands that is composed almost entirely of myoepithelial cells and lacks a ductal/luminal component. Epithelial-myoepithelial carcinoma (EMC) is a biphasic

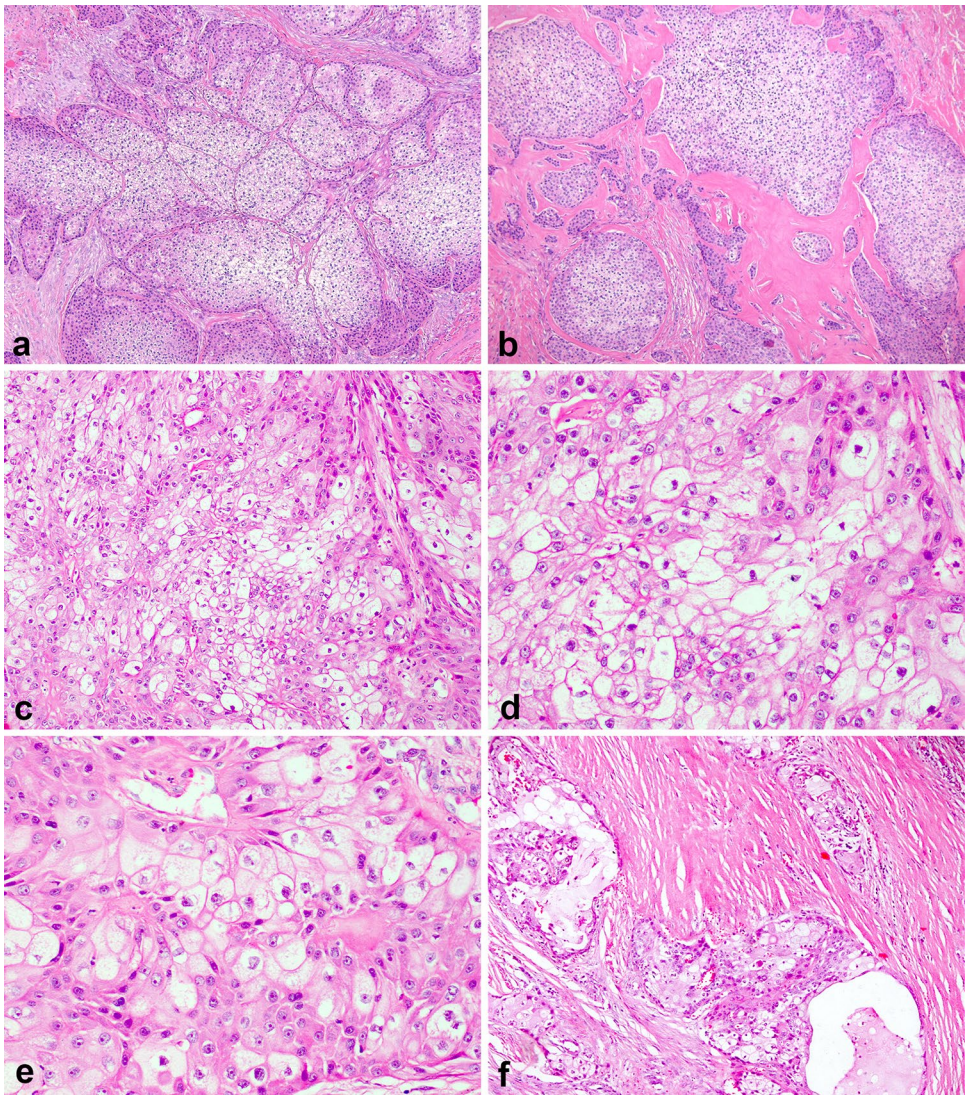

Fig. 3 Clear cell-predominant mucoepidermoid carcinoma can grow in large nests (**a**) with stromal sclerosis reminiscent of hyalinizing clear cell carcinoma (**b**). This mucoepidermoid carcinoma consists predominantly of large polygonal cells with clear cytoplasm (**c**) and small to medium sized nuclei (**d**). Squamoid cells (**e**) and cystic structures containing mucin, focally lined by mucous cells (**f**) are seen in other areas

malignant tumor with inner luminal ductal cells and outer abluminal myoepithelial clear cells. Both tumors are seen most frequently in the parotid gland, followed by minor salivary gland locations [24, 25]. Nearly half of all MEca and EMC are reported to arise ex pleomorphic adenoma [26, 27].

Histologic, Immunohistochemical, and Molecular Findings

Histologically, MEca demonstrates myoepithelial cells with a variety of morphological phenotypes, including epithelioid, spindled, clear, plasmacytoid, and vacuolated (Fig. 4) [24]. These are embedded in a variably myxoid, hyaline, and, rarely, mucinous stroma. An epithelial component, by definition, should be limited to only rare ductal structures, which may show squamous metaplasia. When MEca is composed predominantly of clear cells, it shows nests of polygonal cells with well-defined cytoplasmic borders and round vesicular nuclei; thus, it is not easily distinguished from other clear cell tumors. A helpful feature favoring the diagnosis of MEca over others is a zonation pattern with the tumor being hypercellular at the periphery and hypocellular toward the center. Further, the presence of hyaline droplets of basement membrane material is also characteristic [28]. A minor spindle cell component may be present in clear cell MEca. MEcas have a single cell population immunopositive for keratin and myoepithelial markers including S100 protein (most sensitive), SMA, SOX10, calponin, myosin, GFAP, and p40/p63. Due to variable staining with each of the latter, it is advisable to include more than one myoepithelial marker to confirm the diagnosis of MEca [24].

In EMC, the luminal cells are cuboidal with eosinophilic cytoplasm, while the abluminal myoepithelial cells have clear cytoplasm, more often due to a tissue processing artifact rather than the presence of intracytoplasmic glycogen [25]. In rare double-clear EMCs, accounting for 2–3% of

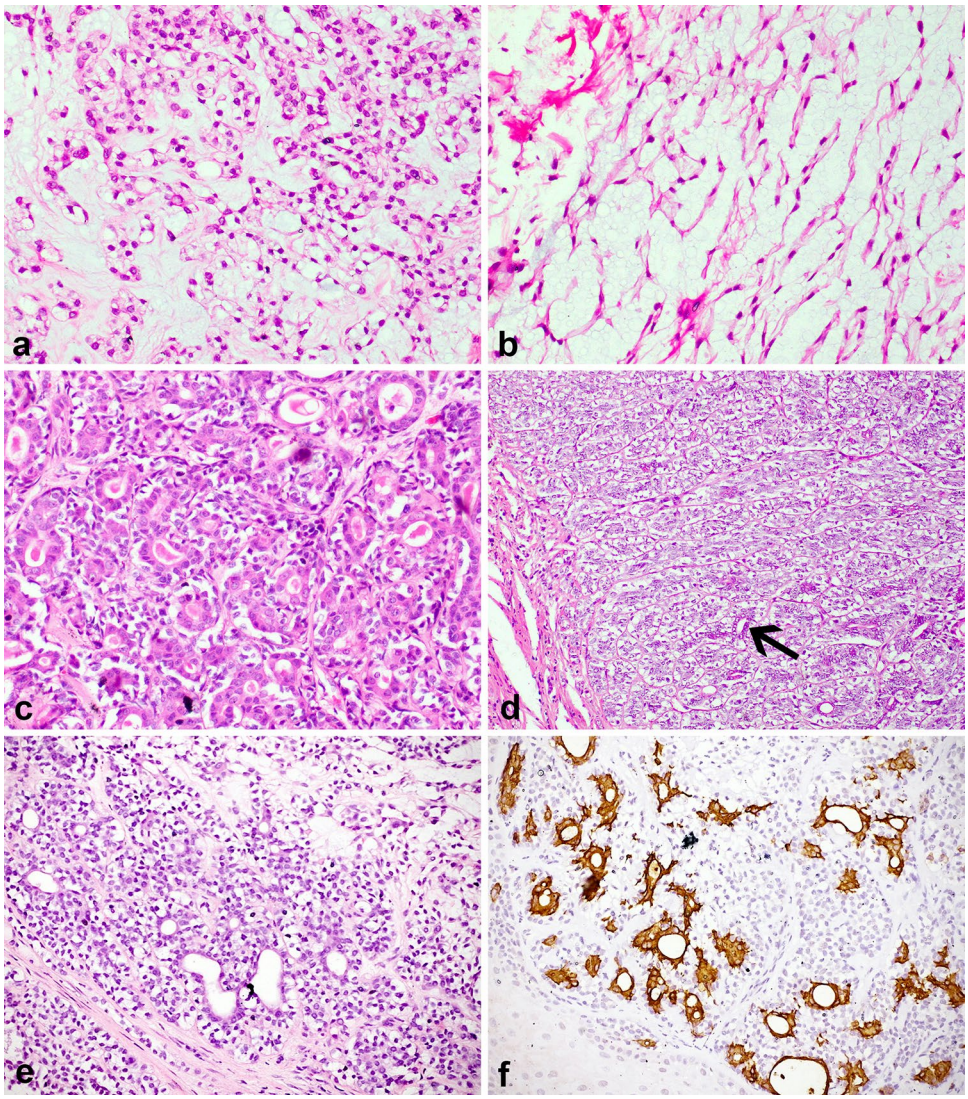

Fig. 4 A myoepithelial carcinoma shows polygonal cells with clear cytoplasm arranged in trabeculae and nests (**a**). Other areas show spindle-shaped tumor cells (**b**). Epithelial-myoepithelial carcinoma (EMC) has a biphasic pattern and clear myoepithelial cells (**c**). Another EMC where almost all cells appear clear and only occasional ductal structures (arrow) are seen (**d**). Pleomorphic adenoma (PA) may contain clear myoepithelial cells (**e**) and ductal structures positive for CK7 (**f**), similar to that seen in EMC. However, circumscription and the presence of chondromyxoid stroma may aid in distinguishing PA from EMC

EMC cases, the luminal cells also have clear cytoplasm. Myoepithelial overgrowth in EMC may lead to areas of the tumor comprised almost entirely of clear myoepithelial cells, mimicking clear cell myoepithelial tumors. In such cases, the biphasic nature of EMC is inconspicuous on hematoxylin and eosin staining, and immunohistochemistry serves to highlight the rare ducts. The luminal/ductal cells stain with CK7, CK19, EMA, CD117, and CEA, while the abluminal/myoepithelial cells are positive for SMA (most sensitive and specific), calponin, S100 protein, SOX10, and p63/p40 (less sensitive and specific) [25].

In summary, MEca is distinguished from EMC based on the biphasic appearance and the presence of ductal structures in the latter. Interestingly, MEca and EMC both harbor *PLAG1* rearrangements, in up to 53% and 33% of cases, respectively [27, 29, 30]. EMC also may show *HMGA2* rearrangement, described in 26% [27]. *HRAS* Q61R mutation is seen in 66% of EMC; when present, it can be detected by immunopositivity for *RAS* Q61R mutant-specific antibody, aiding in diagnosis. Alternatively, *HRAS* mutation can be detected by sequencing.[31].

Differential Diagnosis and Clinical Implications

Differential diagnosis of both MEca and EMC includes pleomorphic adenoma (PA) with clear cells. Although PAs are benign tumors, pseudopods often extend through the capsule and may be seen as satellite nodules outside it. Chondroid stroma is supportive of a PA. Conversely, MEca and EMC generally do not have frankly chondroid stroma. They may have a pseudocapsule with a multilobular pattern of invasion, and the border may not demonstrate small nested infiltration. Additionally, MEca and EMC may have bland cytomorphology, making it hard to characterize them as malignant. *PLAG1* immunohistochemistry and gene rearrangement are not helpful, as a significant proportion of

MEca and EMC arise ex PA, and de novo EMC also demonstrate *PLAG1* or *HMGA2* alterations and immunopositivity, as do benign PAs. HCCC and clear cell MEC are excluded from the differential diagnosis as they lack a myoepithelial cell component, and are therefore immunonegative for myoepithelial-type markers. *EWSR1* rearrangement characteristic of HCCC has also been identified in a subset of MEca enriched for cases with clear cell morphology and associated with poor prognosis [32]. However, the same group subsequently showed that *EWSR1* fusion transcripts were absent on NGS, and suggested that *EWSR1* alterations in MEcas may represent passenger and not driver mutations [30]. Thus, sequencing may be the best molecular technique to distinguish MEca from HCCC. This distinction is clinically relevant as MEca is associated with higher rates of recurrence and metastasis [30].

Clear Cell Oncocytic Lesions of Salivary Gland

Introduction and Epidemiology

Oncocytic lesions of salivary gland (aside from Warthin tumors) may consist of oncocytomas, nodular oncocytic hyperplasia (NOH), or oncocytic metaplasia in other primary salivary-type neoplasms. Oncocytes contain abundant mitochondria, imparting a granular eosinophilic character to the cytoplasm. However, a relative predominance of glycogen in the cytoplasm of such cells confers a clear cytoplasmic appearance [33, 34]. Oncocytomas are thought to represent 1–2% of all salivary neoplasms, most often occur in the parotid gland, and are associated with radiation exposure in up to 20% of patients [35]. Nodular oncocytic hyperplasia occurs overwhelmingly in the parotid gland, either bilaterally or unilaterally, and most often in adults in the 5–6th decades [36]. Clear cell change in such oncocytic lesions can be focal, multifocal, or diffuse, occasionally obscuring their true oncocytic nature.

Histologic, Immunohistochemical, and Molecular Findings

Grossly, oncocytic lesions appear characteristically tan-brown, but clear cell-rich lesions can be increasingly yellow. Clear cell-predominant oncocytomas are well-circumscribed or encapsulated and composed of large cells arranged in nests (occasionally with central cellular dyscohesion creating the appearance of a lumen) surrounded by thin vascular septa (Fig. 5). The extent of clear cell change can range from diffuse to patchy, with some cells retaining eosinophilic cytoplasm, especially adjacent to the cell membrane [33]. Ultrastructurally, mitochondria and other organelles are pushed to the periphery of the cell, but the nuclei remain small, dark, and centrally located [34]. Nodular oncocytosis or NOH consists of variably sized unencapsulated nodules of eosinophilic or clear cell oncocytes sprinkled throughout the gland.

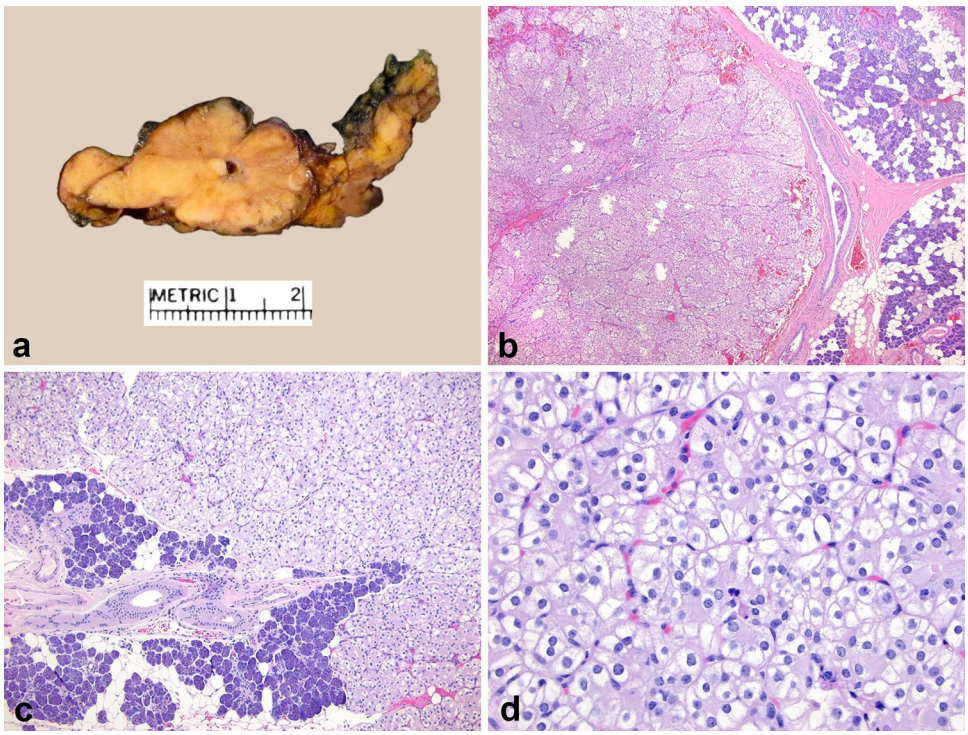

Fig. 5 Grossly, oncocytic salivary neoplasms may appear variably yellow to brown, depending on the ratio of clear to eosinophilic cells, respectively (**a**). This oncocytoma contains an admixture of pale eosinophilic to clear cells in nests (**b**). Nodular oncocytic hyperplasia shows scattered, unencapsulated proliferations of oncocytes throughout salivary parenchyma (**c**). Oncocytic lesions can show cytoplasmic clearing, in this case, with variable amounts of optically clear to pale granular eosinophilic cytoplasm and round nuclei with inconspicuous nucleoli (**d**)

Non-lesional acini, ducts, or fat cells may be entrapped within the nodules. On occasion, a nodule can proliferate to an extent that it appears to represent an oncocytoma arising in oncocytic hyperplasia [36]. In both oncocytomas and NOH, basally located cells are positive for p63 [37]. Genetic drivers remain largely unknown.

Differential Diagnosis and Clinical Implications

The differential diagnosis includes metastatic renal cell carcinoma, which, unlike salivary clear cell oncocytic lesions, would be negative for p63 and positive for PAX8 [37]. Clear cell/oncocyte-rich mucoepidermoid carcinoma would express p63 more diffusely, and the presence of *MAML2* rearrangement would be diagnostic. Clear cell carcinoma would diffusely express p63 and CK5/6, and harbor *EWSR1::ATF1* rearrangement. Additionally, expression of markers of myoepithelial differentiation (S100 protein, SOX10, SMA, calponin) would favor clear cell-rich pleomorphic adenoma or myoepithelioma [23].

Prognostically, most oncocytomas are benign with low likelihoods of recurrence or malignant transformation. NOH has never been reported to transform. However, it has been shown that clear cell phenotype of oncocytic lesions is associated with bilateral disease and recurrence [35].

Glycogenated Squamous Cell Carcinoma

Introduction and Epidemiology

An exhaustive discussion of SCC of the mucosal sites of the head and neck is beyond the scope of this article; however, excessive cytoplasmic glycogen deposition in a SCC may make diagnosis challenging due to morphologic overlap with other carcinomas discussed in this chapter. Clear cell change only occasionally occurs in mucosal SCCs, but is more common in cutaneous SCCs [38–40]. However, due to patterns of lymphatic drainage, head and neck cutaneous SCCs metastasize to intra- and peri-parotid lymph nodes and can mimic primary salivary gland carcinomas [41]. Of all head and neck cutaneous sites, primary carcinomas of the cheek, pinna, temple, and forehead demonstrate the highest rates of metastasis to the parotid gland and its associated lymph nodes [42].

Histologic, Immunohistochemical, and Molecular Findings

Clear cell-rich SCC may, at least focally, retain histologic evidence of squamous differentiation in the form of cytoplasmic keratinization, keratin pearls, and prominent intercellular bridges (Fig. 6). Occasionally, the clear cytoplasm can displace the nucleus so as to resemble an adipocyte or manifest as multiple vacuoles resembling sebaceous cells

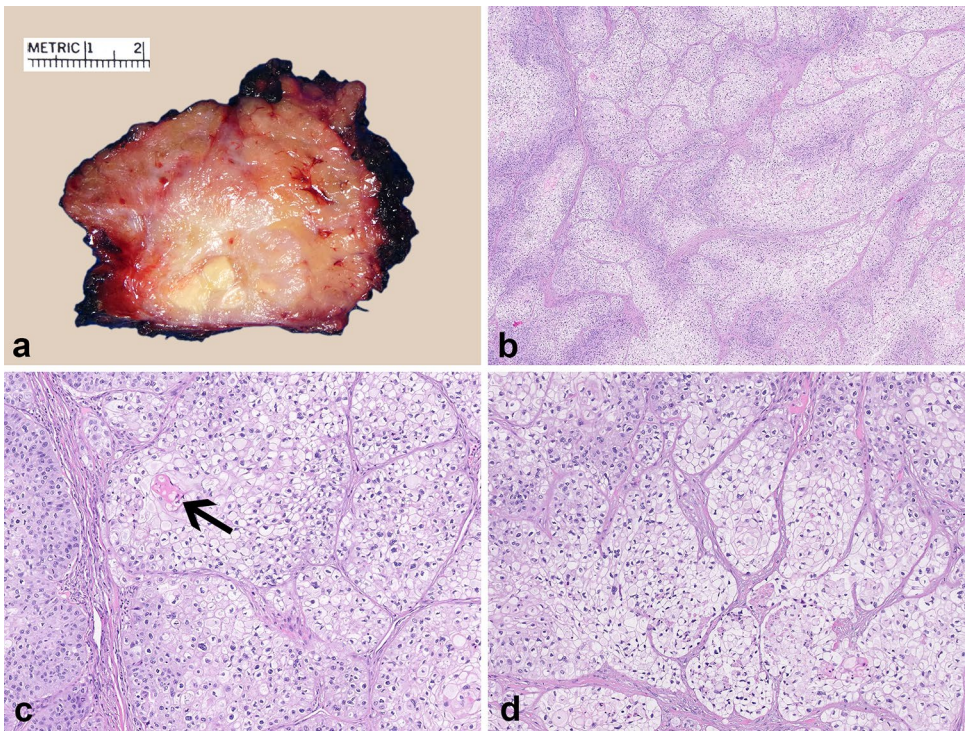

Fig. 6 Metastatic squamous cell carcinoma involving the parotid gland can be grossly infiltrative and demonstrates a firm, white cut surface in contrast to the background lobulated orange-yellow parotid parenchyma (**a**). This carcinoma (a cutaneous metastasis) shows variably sized nests of clear to amphiphilic cells with intervening fibrous bands (**b**). In areas, nests show evidence of squamous differentiation in the form of dense eosinophilic keratin (arrow) (**c**). Cells contain abundant intracytoplasmic glycogen and hyperchromatic nuclei with wrinkled contours (**d**)

[40]. Features of malignancy (infiltrative growth, pleomorphism, mitoses) should be evident. Expression of conventional squamous markers is retained (p63, p40, high molecular weight cytokeratins). In cases of cutaneous carcinomas infiltrating or metastasizing to salivary glands, evidence of sun exposure via ultraviolet (UV) signature mutations can be detected [41].

Differential Diagnosis and Clinical Implications

When present in salivary glands, SCC may mimic HCCC both morphologically and immunohistochemically (both expressing p63, p40, high molecular weight keratins). However, HCCC is often of lower histologic grade (with dark, wrinkled or round nuclei and infrequent mitoses), contains more prominent stromal fibrous bands, lacks a UV signature, and can be confirmed with *EWSR1*::*ATF1* rearrangement [23]. In rare intraparotid SCCs, a site of origin cannot be determined based on UV signature or history, and may represent an undiagnosed mucosal site primary. These patients have been shown to have worse prognosis than those with cutaneous metastases to the parotid gland [41].

Parathyroid Water Clear Cell Adenoma

Introduction and Epidemiology

Parathyroid adenomas account for more than 80% of primary hyperparathyroidism, with a peak incidence in the 5th and 6th decades and a 2:1 female: male ratio [43]. While parathyroid adenomas are most frequently composed of chief cells with an admixture of oncocytic (oxyphil) cells and clear cells, some adenomas (3–6%) are composed entirely of oncocytic cells and rare adenomas are composed entirely of clear cells, so-called water clear cell adenomas (WCCA) [44]. The first case of a solitary parathyroid lesion composed entirely of clear cells was described by Grenko, et al., in 1995, in a patient with hyperparathyroidism [45]. Some studies suggest that water clear cell adenomas have a higher (6:1) female preponderance, larger size, and lower rates of biochemical hyperparathyroidism [46]. Parathyroid adenomas can occur within normally located glands, ectopic glands (including within the thyroid), or supernumerary glands. Additionally, clear cell-predominant lesions can occur in a single gland, two glands, or multiple glands, raising the possibility of multi-gland WCCA versus water clear cell hyperplasia (WCCH) [46, 47]. However, as understanding of the genetic underpinnings of parathyroid disease increases, multiglandular parathyroid disease is being recognized as multi-gland adenomas rather than hyperplasia [44]. Whether the rare multi-gland WCCH represents multi-gland WCCAs or true hyperplasia is yet to be determined.

Histologic, Immunohistochemical, and Molecular Findings

Parathyroid WCCAs consist of nests, cords, or sheets of cells with distinct cell borders and abundant clear or vacuolated cytoplasm (Fig. 7). The nuclei are often located at the basal aspect of the cell. They can be small and hyperchromatic to medium in size with inconspicuous nucleoli. There is delicate stromal vasculature separating nests of tumor cells and minimal to absent stromal fat. A normal, compressed, or atrophic rim of parathyroid tissue (consisting of chief cells admixed with fat) may be present at the periphery, indicating the neoplastic nature of the lesional clear cell population.

Water clear cells express parathyroid hormone (PTH), GATA3, and chromogranin (confirming parathyroid origin) and are negative for calcitonin [46, 48, 49]. While non-clear cell parathyroid adenomas/hyperplasias have been shown to occasionally express TTF1, monoclonal, or polyclonal PAX8, WCCAs have been demonstrated by some authors to be negative for TTF1 and monoclonal PAX8 [46, 50]. Ki67 proliferation index is low (< 2%). Loss of parafibromin (as can be seen in other atypical parathyroid neoplasms, generally with eosinophilic cytoplasm) has not been documented in WCCAs [46, 47, 51]. Electron microscopic examination of the water clear cells demonstrates variably sized membrane-bound vesicles containing flocculent material, dense core granules, and mitochondria [45, 52].

There is limited knowledge of the molecular profile of WCCAs. Conventional chief cell adenomas and WCCAs have been shown to have protein expression patterns more similar to each other than to oxyphilic cell adenomas, and many consider water clear cells as morphologic variants of chief cells [53].

Differential Diagnosis and Clinical Implications

The differential diagnosis of a parathyroid WCCA, especially if closely associated with the thyroid or even intrathyroidal, includes metastatic clear cell RCC, a clear cell thyroid neoplasm, or a medullary thyroid carcinoma. RCC expresses monoclonal PAX8 and CAIX, while parathyroid WCCA does not. Clear cell thyroid neoplasms strongly express monoclonal PAX8, TTF1, and thyroglobulin. Parathyroid WCCAs are negative for thyroglobulin, TTF1, and monoclonal PAX8 (in contrast so some non-clear cell parathyroid lesions which can express TTF1 or PAX8) [50, 54]. A single case of clear cell parathyroid carcinoma has been reported, in this case, mimicking medullary thyroid carcinoma in light of the nested growth pattern, clear to finely vacuolated cytoplasm, and stippled chromatin [55]. The absence of calcitonin expression and the presence of parathyroid immunomarkers are diagnostically useful in cases with this differential diagnostic dilemma.

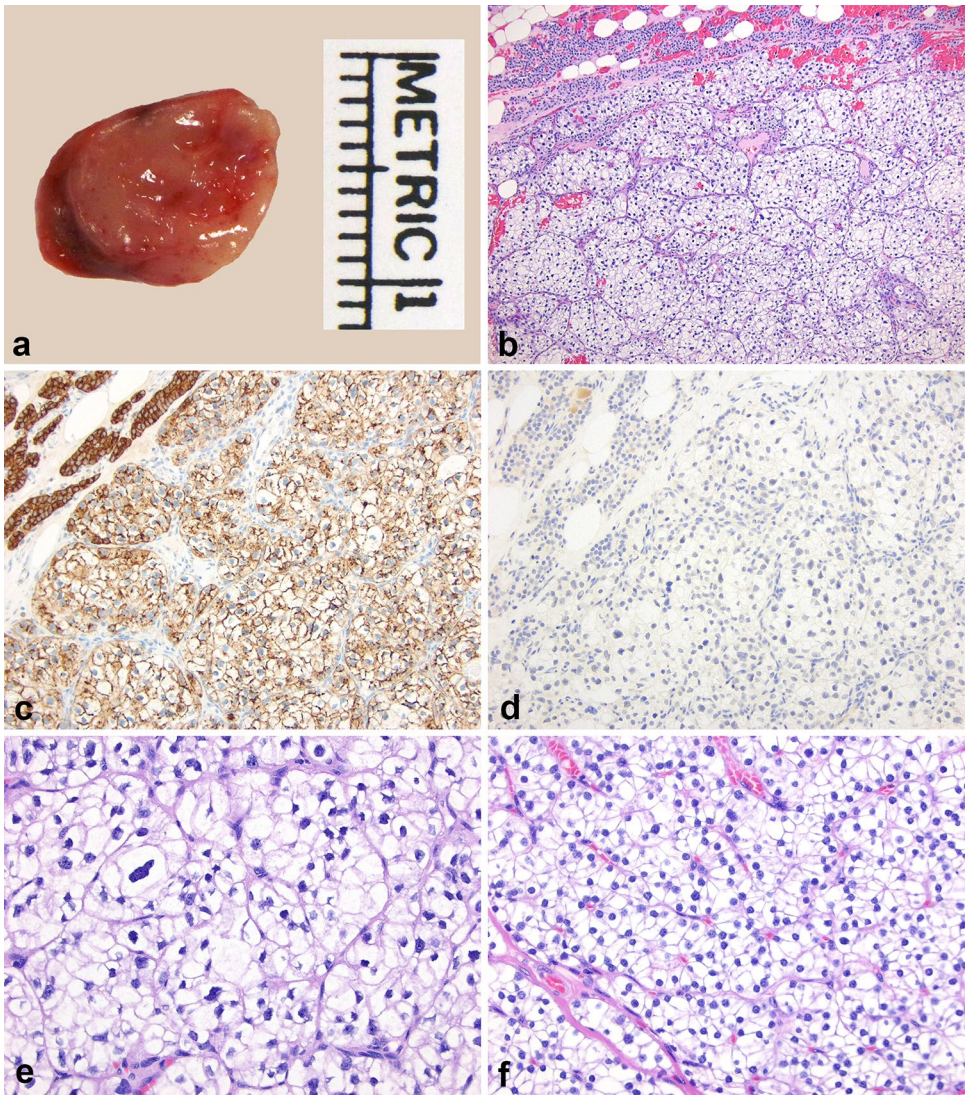

Fig. 7 Grossly, this water clear cell parathyroid adenoma (WCCA) is pale tan-red with a thin, red rim (left side) representing non-neoplastic parenchyma (**a**). The neoplastic cells grow in nests with fine fibrovascular septa and lack of adipose tissue. Background normocellular parenchyma with admixed adipose tissue is in the top left (**b**). Both adenoma cells and non-neoplastic cells are positive for parathyroid hormone (**c**) and negative for monoclonal PAX8 (**d**). WCCA cells have abundant optically clear cytoplasm. Nuclei can vary from enlarged and wrinkled (random endocrine atypia) (e) to small, round, and regular (**f**)

Excision of a WCCA is generally curative. The largest study of such tumors to date has demonstrated that they are often large, biochemically indolent (non- or poorly secreting), and may not be detected with Sestamibi scintigraphy [46].

Metastatic Clear Cell Renal Cell Carcinoma

Introduction and Epidemiology

Renal cell carcinoma (RCC) occasionally metastasizes to the head and neck, with the cervical lymph nodes and thyroid gland the most common sites affected. However, other sites have included the skin, craniofacial bones, sinuses, oral mucosa, and major salivary glands [56–59]. Head and neck metastases have been documented as the initial presentation of occult RCC, discovered at the time of diagnosis of known primary RCC, and as late sequelae of RCC. Males are generally more affected than females. Of patients with RCC, it is estimated that only 1% have metastases confined to the head and neck [58]. Considering metastases to the thyroid gland, RCC (specifically, clear cell type) is the most common (20–30%), followed by carcinomas of the lung, lower gastrointestinal tract, and breast [60–62]. Of all thyroid gland malignancies, metastasis is still very rare (0.36% of malignancies and 0.1% of all neoplasms) [60, 63].

Histologic, Immunohistochemical, and Molecular Findings

The gross appearance of metastatic RCC is bright yellow to orange, similar to primary intrarenal carcinomas. The morphology of clear cell RCC recapitulates that within the kidney: nests and tubules of cells with optically clear cytoplasm and a richly vascular network of stromal capillaries

surrounding tumor cell nests (Fig. 8). Nuclei vary depending on tumor grade and can range from small and round with homogenous chromatin to large and ovoid with variably prominent nucleoli [59]. Regarding intrathyroidal metastases, tumors can be uni- or multifocal, and can occasionally involve pre-existing thyroid gland lesions, including neoplasms. While PAX8 is expressed in tumors of both renal and thyroid origin, TTF1 is negative in RCC and can aid in diagnosis. Additionally, CAIX expression can support clear cell RCC [64]. An exhaustive immunohistochemical and molecular review of renal cell neoplasms is beyond the scope of this article, and readers are referred to other comprehensive resources [64–66].

Differential Diagnosis and Clinical Implications

The differential diagnosis of metastatic clear cell RCC varies depending on metastatic site affected. Within the thyroid gland, considerations include primary thyroid neoplasms with clear cell change (thyroglobulin, PAX8, and TTF1 positive) (Fig. 9a–b) or water clear cell parathyroid adenomas (monoclonal PAX8 and TTF1 negative) [67, 68]. Within the major and minor salivary glands (including oral mucosa) and jaws, clear cell carcinoma of salivary or odontogenic origin may be considered. These tumors would express markers of basaloid/squamoid differentiation (p63, p40, CK5/6), and most harbor *EWSR1*::*ATF1* fusion [23]. Clinically, mean survival time from diagnosis of RCC metastatic to the head and neck has been reported as 38 months (range 12–83 months) [56]. Median survival of RCC metastatic to the thyroid is 20 months (range 3–171 months) in patients who underwent resection versus 12 months (range 1–228 months) in those who did not [61, 63]. Thyroid carcinomas with clear cell change represent a low percentage of all thyroid gland carcinomas (0.5%) and most tend to be *RAS*-like follicular neoplasms [67].

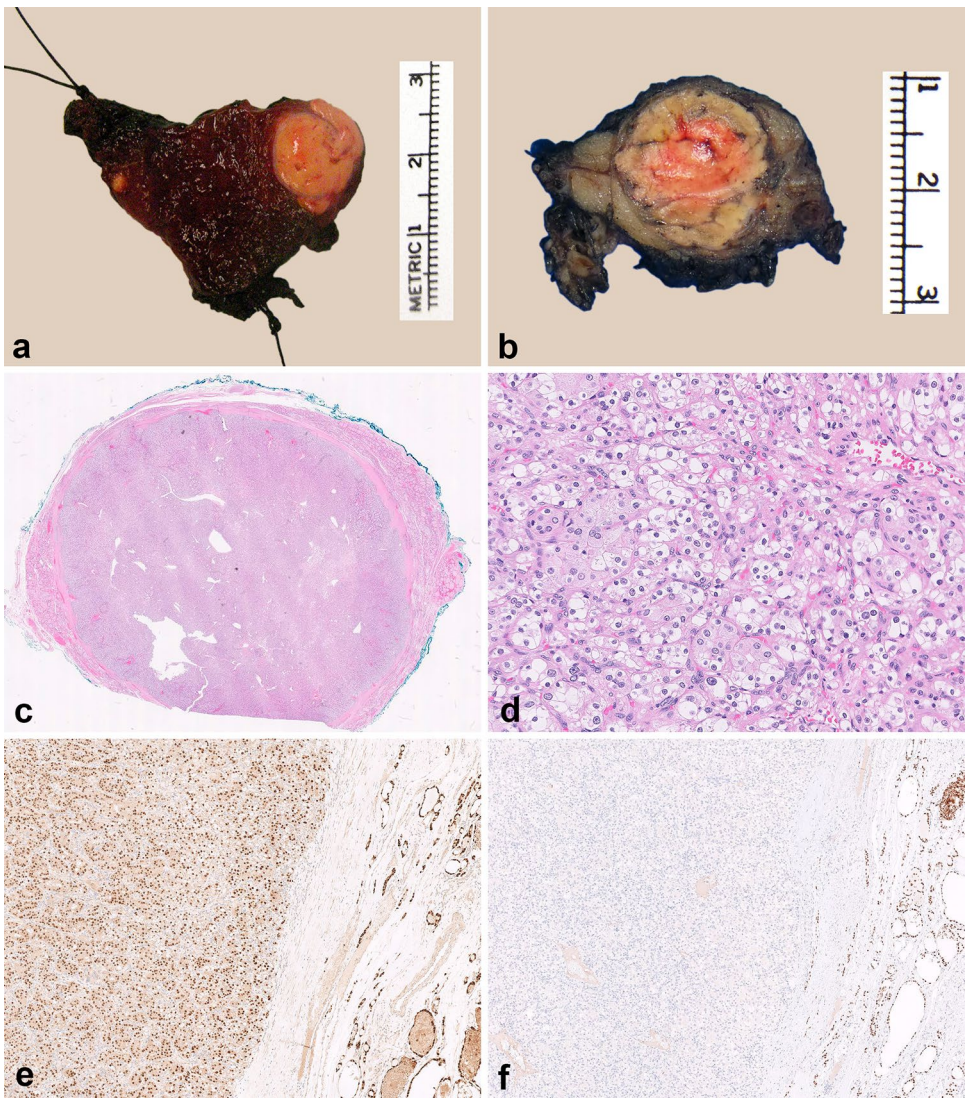

Fig. 8 Metastatic clear cell renal cell carcinoma (RCC) to the thyroid (**a**) or parotid gland (**b**) maintains the characteristic gross yellow-orange appearance of RCC and may be unifocal or multifocal. This intrathyroidal metastasis is circumscribed and can mimic a primary thyroid neoplasm (**c**). Cells are nested with clear to pale eosinophilic cytoplasm (**d**). PAX8 immunostain is positive in the metastasis (left side) and background thyroid parenchyma (right side) (**e**), while TTF1 is only positive in the thyroid parenchyma (**f**)

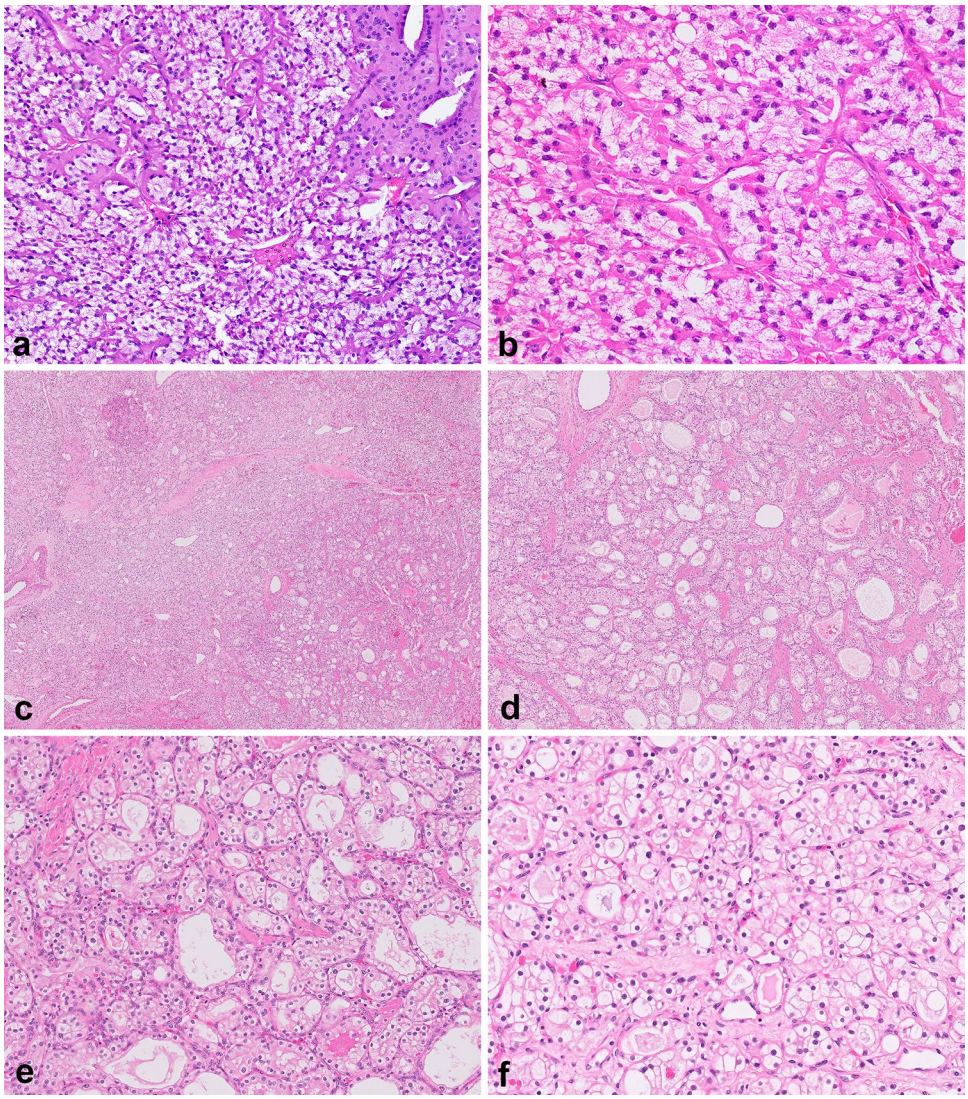

Fig. 9 On occasion, follicular thyroid neoplasms can show prominent clear cell change and can be difficult to distinguish from metastatic renal cell carcinoma (RCC). A conventional oncocytic area is seen in the top right and can point to the underlying thyroid origin of the lesion (**a**). In this thyroid neoplasm, cells are nested with finely granular cytoplasm and there is a paucity of colloid (**b**). Sinonasal renal cell-like adenocarcinoma (SRCLA) is a subtype of sinonasal non-intestinal type adenocarcinoma (**c**). It can grow in small nests and microcysts resembling RCC (**d**). The stroma is collagenous to vascular (**e**) and cells have optically clear cytoplasm with round, dark nuclei (**f**). [Thyroid images contributed by Dr. Shipra Agarwal]

Sinonasal Renal Cell-Like Adenocarcinoma

Introduction and Epidemiology

Sinonasal renal cell-like adenocarcinomas (SRCLA) are a rare subtype of non-intestinal-type sinonasal adenocarcinoma. First described in 2002 as a mimic of RCC metastatic to the sinus [69], RCC is the most common neoplasm to metastasize to this site, followed by lung [70]. However, sinus metastasis is thought to occur in up to 1% of patients with RCC, and may occasionally be the presenting sign of an occult RCC [71]. Discriminating between SRCA and metastatic RCC, even in the absence of a known RCC, is therefore clinically important. Epistaxis is the most common presenting sign in both cases [71, 72].

Histologic, Immunohistochemical, and Molecular Findings

SRCLA is composed of uniform cuboidal cells arranged in a nested and gland-like growth pattern with fibrovascular septae. (Fig. 9c–f) Cytoplasm is abundant and clear to pale eosinophilic without evidence of mucin production. Nuclei are often small and dark with occasional characteristic intranuclear vacuoles or pseudoinclusions [72]. Ultrastructurally, the cytoplasm contains glycogen as well as occasional lipid vacuoles and cholesterol [69]. High grade features (including necrosis, high mitotic activity, perineural or lymphovascular invasion, and significant nuclear pleomorphism) have not been described. Expectedly, these carcinomas are negative for PAX8 and RCC

marker. However, they do express CK7, CAIX, and CD10 [73].

Differential Diagnosis and Clinical Implications

The most salient differential diagnostic consideration, metastatic RCC, can be distinguished from SRCLA based on expression of PAX8, RCC marker, and vimentin and lack of expression of CK7. Unlike clear cell-rich SCC or salivary gland neoplasms (oncocytoma, mucoepidermoid carcinoma, clear cell carcinoma), SRCLA has not been documented to express p63 or smooth muscle actin. SRCLA does not express TTF1, unlike thyroid carcinomas with clear cell change [73]. Clinically, SRCLA has not been shown to recur or metastasize following surgical resection [72, 74]. The genetics remain unknown.

Chordoma

Introduction and Epidemiology

Chordoma is a rare malignant bone tumor that recapitulates the notochord and arises in the axial skeleton at cranial, spinal, and sacrococcygeal sites. A third of all chordomas occur in the skull base (particularly clivus) and cervical spine; rare extra-axial head and neck locations include the nasopharynx, sinonasal tract, oropharynx, and soft tissues of the neck [75]. Chordomas are seen across all age groups, most often between 40 and 60 years of age, with a male preponderance [76, 77]. In children and young adults, skull base chordomas are more common than those at other sites [76, 78]. On imaging, chordomas appear as midline solitary lytic destructive lesions; matrix calcification may be present [79].

Histologic, Immunohistochemical, and Molecular Findings

Grossly, chordomas are solid, lobulated, gelatinous tumors that often extend beyond the cortex of the involved bone into the adjacent soft tissue. Histologically, chordomas are of four subtypes: conventional, chondroid, poorly differentiated, and dedifferentiated (Fig. 10). Conventional chordomas are characterized by tumor lobules separated by fibrous septa, with cords and nests of epithelioid cells with clear vacuolated to pale eosinophilic cytoplasm embedded in a myxoid extracellular matrix [79]. Physaliphorous cells are large, with voluminous bubbly, vacuolated cytoplasm and small hyperchromatic to large vesicular nuclei [78]. Nuclear atypia and pleomorphism may be minimal with only occasional mitoses, to marked with high mitotic activity. Chondroid chordoma contains matrix that closely resembles neoplastic hyaline cartilage [78]. Poorly differentiated chordoma consists predominantly of sheets of epithelioid cells with large vesicular nuclei and prominent nucleoli, with a variable proportion of rhabdoid cells; physaliphorous cells are absent and myxoid stroma is scant [77, 78]. Dedifferentiated chordomas display a high-grade sarcoma juxtaposed with conventional chordoma. Chordomas are immunopositive for keratin, epithelial membrane antigen, S100 protein, and brachyury (encoded by the *TBXT* gene), the latter being most specific. Loss of INI-1 expression is a feature of poorly differentiated chordoma, attributed to homozygous deletion of *SMARCB1*.

Differential Diagnosis and Clinical Implications

Differential diagnoses include chondrosarcoma, myoepithelial tumors of bone and soft tissue (BST), and primary and metastatic carcinomas. While chondroid chordoma mimics classical chondrosarcoma, conventional chordoma can resemble clear cell chondrosarcoma, as the latter consists of cells with abundant clear to pale eosinophilic cytoplasm. Clear cell chondrosarcoma, however, has distinct cytoplasmic borders, and woven bone and osteoclastic giant cells are often present. While chondrosarcomas are also immunopositive for S100 protein and may show keratin and EMA staining, negative brachyury distinguishes them from chordomas; SOX9 may be positive in chordoma and does not help in this differential diagnosis [75]. Although clear cell chondrosarcoma accounts for only 2–3% of all chondrosarcomas, this histologic subtype is associated with significantly worse outcome, warranting its accurate distinction from chordoma [80].

BST myoepithelial tumors, i.e., myoepithelioma and myoepithelial carcinoma, are rare neoplasms that recapitulate the histologic and immunohistochemical features of their salivary gland counterparts. In the head and neck, they have been described in the sinonasal and periorbital regions, and in the clivus [81, 82]. They are composed of epithelioid to spindled cells with clear to eosinophilic cytoplasm embedded in a myxoid, chondromyxoid, or collagenous stroma, rendering considerable similarity to chordoma [82]. Immunohistochemically, they are positive for S100 protein and EMA with variable keratin, GFAP, and myogenic marker expression. A subset of myoepithelial carcinomas show loss of INI-1 expression. Molecular testing may be of value as *EWSR1* or *FUS* rearrangements may be present in BST myoepithelial tumors; of note, *EWSR1*::*POU5F1* fusion is identified in a subset of tumors with predominantly clear cells that occur in children and young adults [81]. Rarely, chordoid meningioma may occur in the skull base, with similar cords of vacuolated cells in a myxoid background, and variably positive keratin and EMA [83]. Admixed foci of classical meningioma, lymphoplasmacytic infiltrate, and immunopositivity for SSTR2A and progesterone receptors

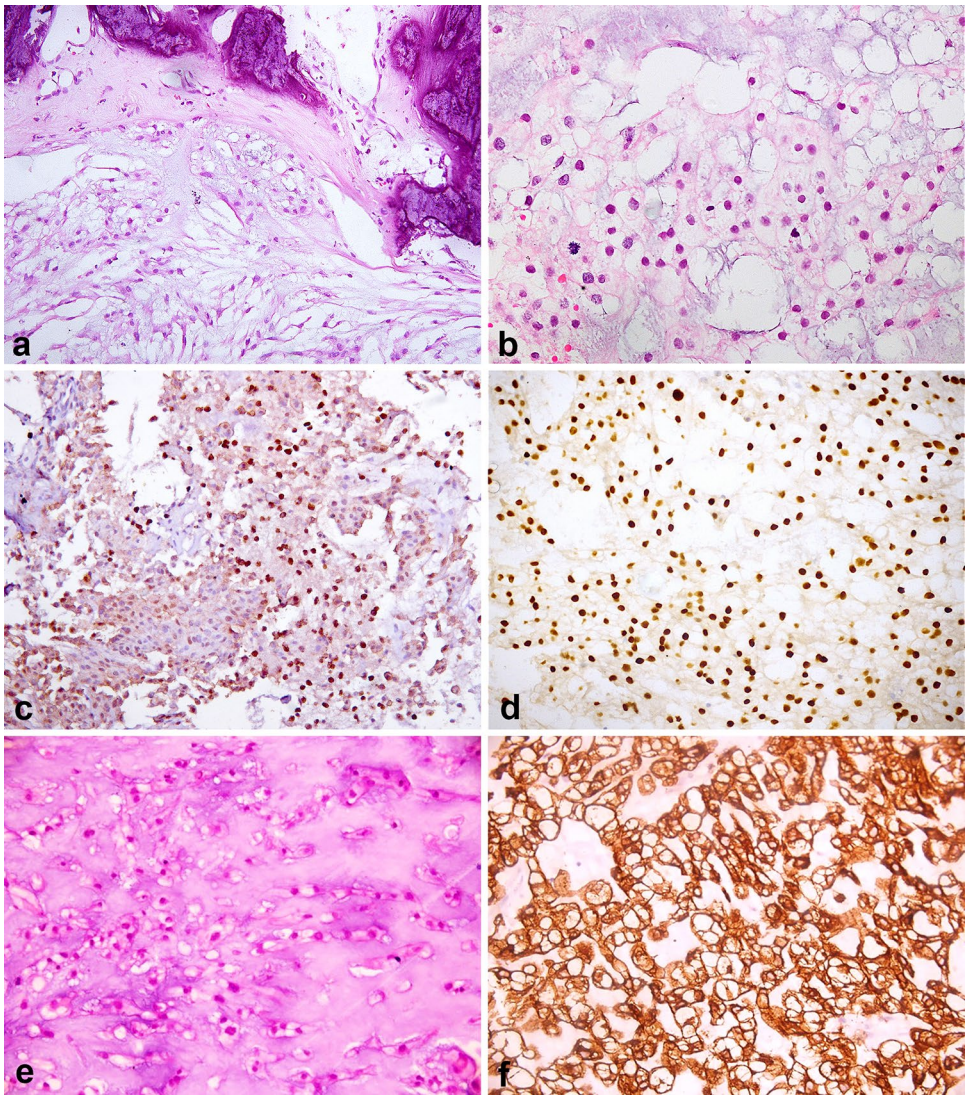

Fig. 10 Conventional chordoma of the clivus is composed of nests of tumor cells destroying bone (**A**). Tumor cells have abundant clear to bubbly vacuolated cytoplasm and small hyperchromatic nuclei with evident mitotic activity (**B**) and show nuclear expression of with S100 protein (**C**) and brachyury (**D**). Chondroid chordoma has abundant matrix that resembles hyaline cartilage (**E**). However, tumor cells are positive for keratin (**F**). [Chondroid chordoma images contributed by Prof. M. C. Sharma]

aid in distinction from chordoma. SRCLA has similar nested cuboidal clear tumor cells but does not have a myxoid matrix and is immunopositive for CAIX and CD10. Brachyury is negative in each of these differential diagnoses, aiding in accurate classification of chordoma.

Rhinoscleroma

Introduction and Epidemiology

Rhinoscleroma is a rare, persistent, progressive chronic infectious granulomatous disease of the upper respiratory tract which is endemic in tropical and sub-tropical countries (Africa, South-East Asia, India, Central and South America, parts of Eastern Europe, and the Middle-East) [84, 85]. Although extremely rare in non-endemic countries, global travel and immigration may lead to its occurrence in non-endemic regions. Rhinoscleroma is caused by *Klebsiella rhinoscleromatis*, a gram-negative bacterium with an airborne route of infection. Socio-economic factors such as malnutrition, poor hygiene, and overcrowding contribute to the spread of disease. It affects a wide age range, however, is most frequent in young adults, with a slight female preponderance. Nasal and nasopharyngeal mucosa are almost always involved; rarely, larynx, trachea, bronchi, palate, nasolacrimal duct, and skin may also be involved [85]. In late stages of infection, patients present with mucosal thickening, hypertrophy, and formation of a locally destructive mass often mimicking malignancy clinically [84].

Histologic, Immunohistochemical, & Molecular Findings

On histology, the initial catarrhal stage shows squamous metaplasia of the nasal mucosa with a neutrophilic

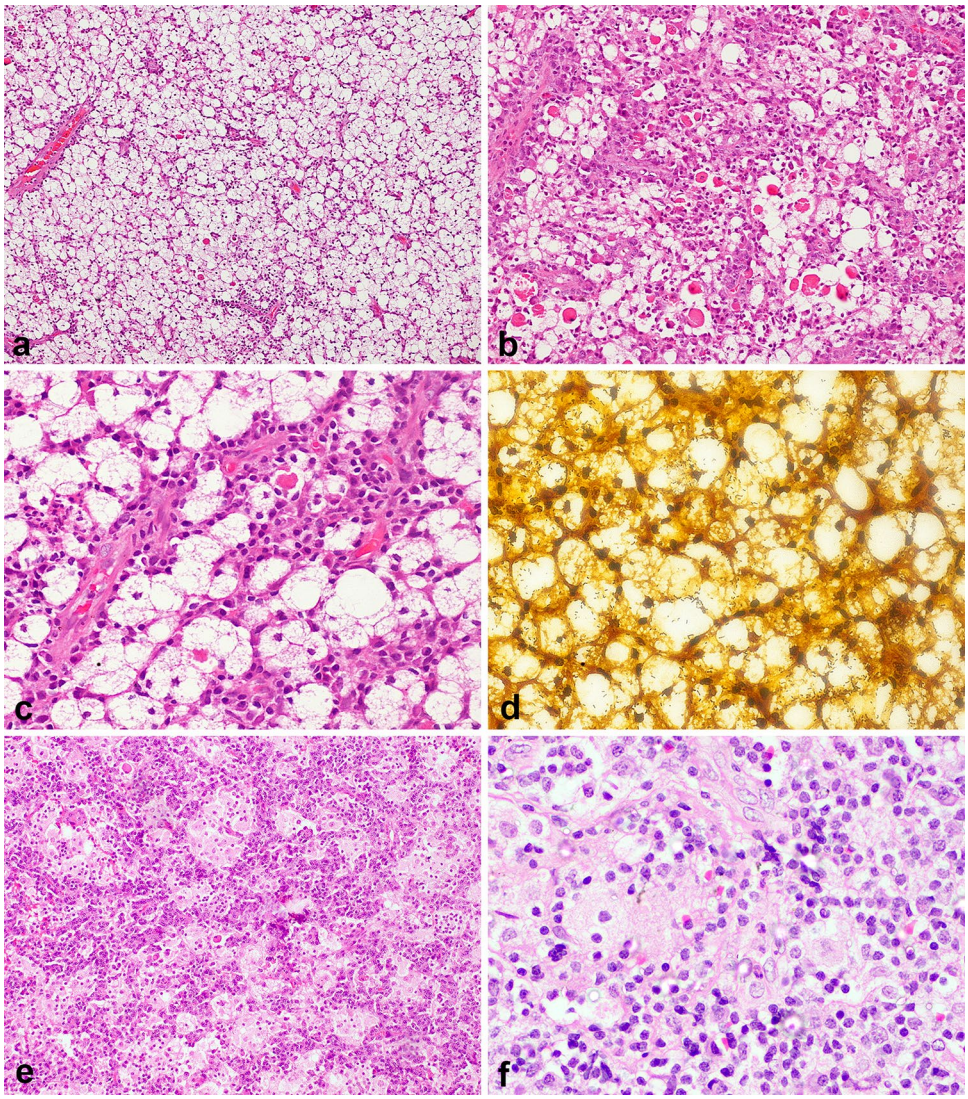

Fig. 11 Rhinoscleroma shows sheets of clear cells interrupted by fibrovascular septa (**A**). Many plasma cells with prominent Russel bodies are seen (**B**). Cells have abundant clear vacuolated to foamy cytoplasm (**C**) and demonstrate intracellular bacilli on Warthin-Starry stain (**D**). Histiocytes in Rosai-Dorfman disease have pale pink, foamy cytoplasm (**E**) and may demonstrate emperipolesis (**F**)

infiltrate; however, this is rarely biopsied (Fig. 11). The hypertrophic stage is characterized by the pathognomonic Mikulicz cells: large, mononuclear cells with clear vacuolated or foamy cytoplasm and peripheral nuclei, often arranged in a nested pattern, and accompanied by a plasma cell-rich infiltrate with easily identifiable Russel bodies, lymphocytes, and a few neutrophils. Mikulicz cells contain numerous gram-negative bacilli, highlighted by Giemsa, Warthin-Starry, and Steiner stains [84]. Immunohistochemistry for Klebsiella antigens may also be performed. Culture studies, PCR-based assays, and 16 s rRNA gene sequencing can detect the organism in tissue culture or nasal swabs for confirmation of diagnosis. Systemic antibiotics and surgical debridement are mainstays of treatment.

Differential Diagnosis and Clinical Implications

Differential diagnosis includes histiocyte-rich lesions, as well as neoplasms with clear cells. Rosai-Dorfman disease (RDD) may involve the sinonasal tract and shows a histiocyte- and plasma cell-rich infiltrate. Emperipolesis, a characteristic feature of nodal RDD, is often absent at extranodal sites, and has also been described in rhinoscleroma [86]. The histiocytes in RDD are immunopositive for S100 protein, while Mikulicz cells are negative. Lepromatous leprosy also shows sheets of foamy histiocytes, lacks the presence of plasma cells, and shows numerous intracytoplasmic acid-fast bacilli. Rhinoscleroma can easily be distinguished from neoplasms with clear cells (e.g., myoepithelioma, CCC, and MEC), as the neoplasms are immunopositive for keratins.

Conclusions

Optically clear cytoplasm may occur in neoplastic and non-neoplastic conditions, either as a characteristic feature of a disease entity or as a morphologic rarity, potentially creating diagnostic dilemmas in various organ systems [1, 2]. [1–6] Overlapping morphologic features may present a diagnostic challenge in surgical pathology material. This review elaborates the top ten clear cell lesions in the head and neck, emphasizing their distinguishing histologic, immunohistochemical, and molecular attributes, and presents a rational approach to arriving at an accurate diagnosis. These top ten lesions are as follows: (1) clear cell carcinoma (salivary gland and odontogenic), (2) mucoepidermoid carcinoma, (3) myoepithelial and epithelial-myoepithelial carcinoma, (4) oncocytic salivary gland lesions, (5) squamous cell carcinoma, (6) parathyroid water clear cell adenoma, (7) metastatic renal cell carcinoma (especially in comparison to clear cell thyroid neoplasms), (8) sinonasal renal cell-like adenocarcinoma, (9) chordoma, and (10) rhinoscleroma (Table 1, Fig. 1).

Author Contributions NAC and AK both contributed meaningfully to conceptualization, manuscript preparation, and finalization.

Funding The authors did not receive support from any organization for the submitted work.

Data Availability Not applicable (no data).

Code Availability Not applicable.

Declarations

Competing interests All authors certify that they have no affiliations with or involvement in any organization or entity with any financial interest or non-financial interest in the subject matter or materials discussed in this manuscript.

Ethical Approval As no human subjects are included in this review article, no ethical approval or Institutional Review Board was required. Consent to participate was waived as this is a review article exclusively. Consent for publication was obtained from all individuals for whom identifying information is uniquely included in this manuscript.

Consent to Participate Not applicable.

Consent for Publication NAC and AK both consent to publication of manuscript.

References

1. Said-Al-Naief N, Klein MJ (2008) Clear cell entities of the head and neck: a selective review of clear cell tumors of the salivary glands. Head Neck Pathol 2:111–115. https://doi.org/10.1007/s12105-008-0052-7
2. Maiorano E, Altini M, Favia G (1997) Clear cell tumors of the salivary glands, jaws, and oral mucosa. Semin Diagn Pathol 14:203–212
3. Eversole LR (1993) On the differential diagnosis of clear cell tumours of the head and neck. Eur J Cancer B Oral Oncol 29:173–179. https://doi.org/10.1016/0964-1955(93)90019-B
4. Skalova A, Leivo I, Hellquist H, Simpson RHW, vander Poorten V, Willems SM, Mosaieby E, Slouka D, Ferlito A (2022) Clear cell neoplasms of salivary glands: a diagnostic challenge. Adv Anat Pathol 29:217–226. https://doi.org/10.1097/PAP.0000000000000339
5. Premalatha B, Neethi H (2012) Clear cell tumors of the head and neck: an overview. World J Dent 3:344–349. https://doi.org/10.5005/jp-journals-10015-1187
6. Kar A, Pattnaik K, Kar T, Biswal P, Mishra C, Clear GL (2020) cell lesions in pathology: histomorphologic approach to diagnosis. Indian J Pathol Microbiol 63:177–187. https://doi.org/10.4103/IJPM.IJPM_791_19
7. Weinreb I (2013) Hyalinizing clear cell carcinoma of salivary gland: a review and update. Head Neck Pathol 7(Suppl 1):S20–S29. https://doi.org/10.1007/s12105-013-0466-8
8. Guastaldi FPS, Faquin WC, Gootkind F, Hashemi S, August M, Iafrate AJ, Rivera MN, Kaban LB, Jaquinet A, Troulis MJ (2019) Clear cell odontogenic carcinoma: a rare jaw tumor. A summary of 107 reported cases. Int J Oral Maxillofac Surg 48:1405–1410. https://doi.org/10.1016/j.ijom.2019.05.006
9. Desai A, Faquin WC, Iafrate AJ, Rivera MN, Jaquinet A, Troulis MJ (2022) Clear cell carcinoma: a comprehensive literature review of 254 cases. Int J Oral Maxillofac Surg 51:705–712. https://doi.org/10.1016/j.ijom.2021.03.018
10. Bishop JA, Rooper LM, Chiosea SI, Westra WH (2018) Clear cell carcinoma of salivary glands is frequently p16 positive: a pitfall in the interpretation of oropharyngeal biopsies. Am J Surg Pathol 42:367–371. https://doi.org/10.1097/PAS.0000000000000977
11. Antonescu CR, Katabi N, Zhang L, Sung YS, Seethala RR, Jordan RC, Perez-Ordoñez B, Have C, Asa SL, Leong IT, Bradley G, Klieb H, Weinreb I (2011) EWSR1-ATF1 fusion is a novel and consistent finding in hyalinizing clear-cell carcinoma of salivary gland. Genes Chromosomes Cancer 50:559–570. https://doi.org/10.1002/gcc.20881
12. Bilodeau EA, Weinreb I, Antonescu CR, Zhang L, Dacic S, Muller S, Barker B, Seethala RR (2013) Clear cell odontogenic carcinomas show EWSR1 rearrangements: a novel finding and a biological link to salivary clear cell carcinomas. Am J Surg Pathol 37:1001–1005. https://doi.org/10.1097/PAS.0b013e31828a6727
13. Rivera CM, Faquin WC, Thierauf J, Afrogheh AH, Jaquinet A, Iafrate AJ, Rivera MN, Troulis MJ (2022) Detection of EWSR1 fusions in CCOC by targeted RNA-seq. Oral Surg Oral Med Oral Pathol Oral Radiol 134:240–244. https://doi.org/10.1016/j.oooo.2021.12.127
14. Siriwardena BSMS, Speight PM, Franklin CD, Abdelkarim R, Khurram SA, Hunter KD (2021) CEOT variants or entities: Time for a Rethink? A case series with review of the literature. Head Neck Pathol 15:186–201. https://doi.org/10.1007/s12105-020-01200-9
15. Mosqueda-Taylor A, Neville BW, Tatemoto Y, Ogawa I, Takata T (2014) Odontogenic carcinoma with dentinoid: a new odontogenic carcinoma. Head Neck Pathol 8:421–431. https://doi.org/10.1007/s12105-014-0586-9
16. Gondak RO, Mariano FV, de Sousa SF, de Siqueira EC, Díaz KP, Martins LAL, Altemani A, Mosqueda-Taylor A, Gomes RS, Gomes CC (2020) CTNNB1 and APC mutations in odontogenic carcinoma with dentinoid. Oral Surg Oral Med Oral Pathol Oral

Radiol 129:e249–e256. https://doi.org/10.1016/j.oooo.2019.08.017
17. Nakano S, Okumura Y, Murase T, Nagao T, Kusafuka K, Urano M, Yamamoto H, Kano S, Tsukahara K, Okami K, Kawakita D, Nagao T, Hanai N, Iwai H, Kawata R, Tada Y, Nibu K-I, Inagaki H (2022) Salivary mucoepidermoid carcinoma: histological variants, grading systems, CRTC1/3-MAML2 fusions, and clinicopathological features. Histopathology 80:729–735. https://doi.org/10.1111/his.14586
18. Pires FR, Azevedo RS, Ficarra G, Cardoso AS, Carlos R, Kowalski LP, de Almeida OP (2010) Metastatic renal cell carcinoma to the oral cavity and clear cell mucoepidermoid carcinoma: comparative clinicopathologic and immunohistochemical study. Oral Surg Oral Med Oral Pathol Oral Radiol Endod 109:e22–e27. https://doi.org/10.1016/j.tripleo.2009.12.006
19. Coca-Pelaz A, Rodrigo JP, Triantafyllou A, Hunt JL, Rinaldo A, Strojan P, Haigentz M, Mendenhall WM, Takes RP, vander Poorten V, Ferlito A (2015) Salivary mucoepidermoid carcinoma revisited. Eur Arch Otorhinolaryngol 272:799–819. https://doi.org/10.1007/s00405-014-3053-z
20. Tajima S, Namiki I, Koda K (2017) A clear cell variant of mucoepidermoid carcinoma harboring CRTC1-MAML2 fusion gene found in buccal mucosa: report of a case showing a large clear cell component and lacking typical epidermoid cells and intermediate cells. Med Mol Morphol 50:117–121. https://doi.org/10.1007/s00795-015-0120-5
21. Yang S, Chen X (2010) Calcifications in clear cell mucoepidermoid carcinomas. Oral Surg Oral Med Oral Pathol Oral Radiol Endod 109:274–275. https://doi.org/10.1016/j.tripleo.2009.08.012
22. Cipriani NA, Lusardi JJ, McElherne J, Pearson AT, Olivas AD, Fitzpatrick C, Lingen MW, Blair EA (2019) Mucoepidermoid carcinoma: a comparison of histologic grading systems and relationship to MAML2 rearrangement and prognosis. Am J Surg Pathol 43:885–897. https://doi.org/10.1097/PAS.0000000000001252
23. Higgins KE, Cipriani NA (2022) Practical immunohistochemistry in the classification of salivary gland neoplasms. Semin Diagn Pathol 39:17–28. https://doi.org/10.1053/j.semdp.2021.10.004
24. Xu B, Katabi N (2021) Myoepithelial carcinoma. Surg Pathol Clin 14:67–73. https://doi.org/10.1016/j.path.2020.09.008
25. Nakaguro M, Nagao T (2021) Epithelial-Myoepithelial carcinoma. Surg Pathol Clin 14:97–109. https://doi.org/10.1016/j.path.2020.10.002
26. Kong M, Drill EN, Morris L, West L, Klimstra D, Gonen M, Ghossein R, Katabi N (2015) Prognostic factors in myoepithelial carcinoma of salivary glands: a clinicopathologic study of 48 cases. Am J Surg Pathol 39:931–938. https://doi.org/10.1097/PAS.0000000000000452
27. el Hallani S, Udager AM, Bell D, Fonseca I, Thompson LDR, Assaad A, Agaimy A, Luvison AM, Miller C, Seethala RR, Chiosea S (2018) Epithelial-myoepithelial carcinoma: frequent morphologic and molecular evidence of preexisting pleomorphic adenoma, common HRAS mutations in PLAG1-intact and HMGA2-intact cases, and occasional TP53, FBXW7, and SMARCB1 alterations in high-grade cases. Am J Surg Pathol 42:18–27. https://doi.org/10.1097/PAS.0000000000000933
28. Michal M, Skálová A, Simpson RH, Rychterová V, Leivo I (1996) Clear cell malignant myoepithelioma of the salivary glands. Histopathology 28:309–315. https://doi.org/10.1046/j.1365-2559.1996.d01-439.x
29. Dalin MG, Katabi N, Persson M, Lee K-W, Makarov V, Desrichard A, Walsh LA, West L, Nadeem Z, Ramaswami D, Havel JJ, Kuo F, Chadalavada K, Nanjangud GJ, Ganly I, Riaz N, Ho AL, Antonescu CR, Ghossein R, Stenman G, Chan TA, Morris LGT (2017) Multi-dimensional genomic analysis of myoepithelial carcinoma identifies prevalent oncogenic gene fusions. Nat Commun 8:1197. https://doi.org/10.1038/s41467-017-01178-z
30. Skálová A, Agaimy A, Vanecek T, Baněčková M, Laco J, Ptáková N, Šteiner P, Majewska H, Biernat W, Corcione L, Eis V, Koshyk O, Vondrák J, Michal M, Leivo I (2021) Molecular profiling of clear cell myoepithelial carcinoma of salivary glands With EWSR1 rearrangement identifies frequent PLAG1 gene fusions But No EWSR1 fusion transcripts. Am J Surg Pathol 45:1–13. https://doi.org/10.1097/PAS.0000000000001591
31. Nakaguro M, Tanigawa M, Hirai H, Yamamoto Y, Urano M, Takahashi RH, Sukeda A, Okumura Y, Honda S, Tasaki K, Shimizu A, Tsukahara K, Tada Y, Matsubayashi J, Faquin WC, Sadow PM, Nagao T (2021) The diagnostic utility of RAS Q61R mutation-specific immunohistochemistry in epithelial-myoepithelial carcinoma. Am J Surg Pathol 45:885–894. https://doi.org/10.1097/PAS.0000000000001673
32. Skálová A, Weinreb I, Hyrcza M, Simpson RHW, Laco J, Agaimy A, Vazmitel M, Majewska H, Vanecek T, Talarčik P, Manajlovic S, Losito SN, Šteiner P, Klimkova A, Michal M (2015) Clear cell myoepithelial carcinoma of salivary glands showing EWSR1 rearrangement. Am J Surg Pathol 39:338–348. https://doi.org/10.1097/PAS.0000000000000364
33. Ellis GL (1988) "Clear cell" oncocytoma of salivary gland. Hum Pathol 19:862–867. https://doi.org/10.1016/s0046-8177(88)80271-5
34. Davy CL, Dardick I, Hammond E, Thomas MJ (1994) Relationship of clear cell oncocytoma to mitochondrial-rich (typical) oncocytomas of parotid salivary gland. Oral Surg Oral Med Oral Pathol 77:469–479. https://doi.org/10.1016/0030-4220(94)90226-7
35. Brandwein MS, Huvos AG (1991) Oncocytic tumors of major salivary glands. A study of 68 cases with follow-up of 44 patients. Am J Surg Pathol 15:514–528. https://doi.org/10.1097/00000478-199106000-00002
36. Palmer TJ, Gleeson MJ, Eveson JW, Cawson RA (1990) Oncocytic adenomas and oncocytic hyperplasia of salivary glands: a clinicopathological study of 26 cases. Histopathology 16:487–493. https://doi.org/10.1111/j.1365-2559.1990.tb01549.x
37. McHugh JB, Hoschar AP, Dvorakova M, Parwani A, v, Barnes EL, Seethala RR, (2007) p63 immunohistochemistry differentiates salivary gland oncocytoma and oncocytic carcinoma from metastatic renal cell carcinoma. Head Neck Pathol 1:123–131. https://doi.org/10.1007/s12105-007-0031-4
38. Sahni P, Sinha N, Kumar R, Sharma A (2019) Clear cell variant of Oral squamous cell carcinoma. J Exp Ther Oncol 13:159–163
39. Khoury ZH, Bugshan A, Lubek JE, Papadimitriou JC, Basile JR, Younis RH (2017) Glycogen-rich clear cell squamous cell carcinoma originating in the oral cavity. Head Neck Pathol 11:552–560. https://doi.org/10.1007/s12105-017-0812-3
40. Kuo T (1980) Clear cell carcinoma of the skin. A variant of the squamous cell carcinoma that simulates sebaceous carcinoma. Am J Surg Pathol 4:573–583. https://doi.org/10.1097/00000478-198012000-00008
41. Fishbach S, Steinhardt G, Zhen CJ, Puranik R, Segal JP, Cipriani NA (2022) High rates of ultraviolet-signature mutations in squamous cell carcinomas of the parotid gland and prognostic implications. Head Neck Pathol 16:236–247. https://doi.org/10.1007/s12105-021-01349-x
42. Vauterin TJ, Veness MJ, Morgan GJ, Poulsen MG, O'Brien CJ (2006) Patterns of lymph node spread of cutaneous squamous cell carcinoma of the head and neck. Head Neck 28:785–791. https://doi.org/10.1002/hed.20417
43. Guilmette J, Sadow PM (2019) Parathyroid pathology. Surg Pathol Clin 12:1007–1019. https://doi.org/10.1016/j.path.2019.08.006
44. Erickson LA, Mete O, Juhlin CC, Perren A, Gill AJ (2022) Overview of the 2022 WHO classification of parathyroid tumors. Endocr Pathol 33:64–89. https://doi.org/10.1007/s12022-022-09709-1

45. Grenko RT, Anderson KM, Kauffman G, Abt AB (1995) Water-clear cell adenoma of the parathyroid. A case report with immunohistochemistry and electron microscopy. Arch Pathol Lab Med 119:1072–1074
46. Juhlin CC, Nilsson I-L, Falhammar H, Zedenius J (2021) Institutional characterisation of water clear cell parathyroid adenoma: a rare entity often unrecognised by TC-99m-sestamibi scintigraphy. Pathology 53:852–859. https://doi.org/10.1016/j.pathol.2021.02.011
47. Bai S, LiVolsi VA, Fraker DL, Bing Z (2012) Water-clear parathyroid adenoma: report of two cases and literature review. Endocr Pathol 23:196–200. https://doi.org/10.1007/s12022-012-9211-1
48. Erickson LA, Mete O (2018) Immunohistochemistry in diagnostic parathyroid pathology. Endocr Pathol 29:113–129. https://doi.org/10.1007/s12022-018-9527-6
49. Oliveira AM, Tazelaar HD, Myers JL, Erickson LA, Lloyd Rv (2001) Thyroid transcription factor-1 distinguishes metastatic pulmonary from well-differentiated neuroendocrine tumors of other sites. Am J Surg Pathol 25:815–819. https://doi.org/10.1097/00000478-200106000-00015
50. Altınay S, Erözgür B, Dural AC, Volante M, Papotti MG (2021) Monoclonal/polyclonal PAX-8, PTH and GATA3 immunohistochemistry in parathyroid lesions. J Endocrinol Invest 44:1997–2008. https://doi.org/10.1007/s40618-021-01518-3
51. Gill AJ, Lim G, Cheung VKY, Andrici J, Perry-Keene JL, Paik J, Sioson L, Clarkson A, Sheen A, Luxford C, Elston MS, Meyer-Rochow GY, Nano MT, Kruijff S, Engelsman AF, Sywak M, Sidhu SB, Delbridge LW, Robinson BG, Marsh DJ, Toon CW, Chou A, Clifton-Bligh RJ (2019) Parafibromin-deficient (HPT-JT Type, CDC73 Mutated) parathyroid tumors demonstrate distinctive morphologic features. Am J Surg Pathol 43:35–46. https://doi.org/10.1097/PAS.0000000000001017
52. Sheldon H (1964) on the water-clear cell in the human parathyroid gland. J Ultrastruct Res 10:377–383. https://doi.org/10.1016/s0022-5320(64)80016-2
53. Lu M, Kjellin H, Fotouhi O, Lee L, Nilsson I-L, Haglund F, Höög A, Lehtiö J, Larsson C (2018) Molecular profiles of oxyphilic and chief cell parathyroid adenoma. Mol Cell Endocrinol 470:84–95. https://doi.org/10.1016/j.mce.2017.10.001
54. Cimino-Mathews A, Sharma R, Netto GJ (2011) Diagnostic use of PAX8, CAIX, TTF-1, and TGB in metastatic renal cell carcinoma of the thyroid. Am J Surg Pathol 35:757–761. https://doi.org/10.1097/PAS.0b013e3182147fa8
55. Khalil M, Zafereo M, Gule-Monroe M, Sherman SI, Bell D (2021) Non-functional water clear cell parathyroid carcinoma masquerading as medullary thyroid carcinoma. Ann Diagn Pathol 54:151791. https://doi.org/10.1016/j.anndiagpath.2021.151791
56. Lieder A, Guenzel T, Lebentrau S, Schneider C, Franzen A (2017) Diagnostic relevance of metastatic renal cell carcinoma in the head and neck: an evaluation of 22 cases in 671 patients. Int Braz J Urol 43:202–208. https://doi.org/10.1590/S1677-5538.IBJU.2015.0665
57. Langille G, Taylor SM, Bullock MJ (2008) Metastatic renal cell carcinoma to the head and neck: summary of 21 cases. J Otolaryngol Head Neck Surg 37:515–521
58. Pritchyk KM, Schiff BA, Newkirk KA, Krowiak E, Deeb ZE (2002) Metastatic renal cell carcinoma to the head and neck. Laryngoscope 112:1598–1602. https://doi.org/10.1097/00005537-200209000-00012
59. Majewska H, Skálová A, Radecka K, Stodulski D, Hyrcza M, Stankiewicz C, Biernat W (2016) Renal clear cell carcinoma metastasis to salivary glands - a series of 9 cases: clinico-pathological study. Pol J Pathol 67:39–45. https://doi.org/10.5114/pjp.2016.59475
60. Ghossein CA, Khimraj A, Dogan S, Xu B (2021) Metastasis to the thyroid gland: a single-institution 16-year experience. Histopathology 78:508–519. https://doi.org/10.1111/his.14246
61. Hegerova L, Griebeler ML, Reynolds JP, Henry MR, Gharib H (2015) Metastasis to the thyroid gland: report of a large series from the Mayo clinic. Am J Clin Oncol 38:338–342. https://doi.org/10.1097/COC.0b013e31829d1d09
62. Moghaddam PA, Cornejo KM, Khan A (2013) Metastatic carcinoma to the thyroid gland: a single institution 20-year experience and review of the literature. Endocr Pathol 24:116–124. https://doi.org/10.1007/s12022-013-9257-8
63. Heffess CS, Wenig BM, Thompson LD (2002) Metastatic renal cell carcinoma to the thyroid gland: a clinicopathologic study of 36 cases. Cancer 95:1869–1878. https://doi.org/10.1002/cncr.10901
64. Akgul M, Williamson SR (2022) Immunohistochemistry for the diagnosis of renal epithelial neoplasms. Semin Diagn Pathol 39:1–16. https://doi.org/10.1053/j.semdp.2021.11.001
65. Mohanty SK, Lobo A, Cheng L (2022) The 2022 revision of World Health Organization classification of tumors of the urinary system and male genital organs: advances and challenges. Hum Pathol. https://doi.org/10.1016/j.humpath.2022.08.006
66. Trpkov K, Hes O, Williamson SR, Adeniran AJ, Agaimy A, Alaghehbandan R, Amin MB, Argani P, Chen Y-B, Cheng L, Epstein JI, Cheville JC, Comperat E, da Cunha IW, Gordetsky JB, Gupta S, He H, Hirsch MS, Humphrey PA, Kapur P, Kojima F, Lopez JI, Maclean F, Magi-Galluzzi C, McKenney JK, Mehra R, Menon S, Netto GJ, Przybycin CG, Rao P, Rao Q, Reuter VE, Saleeb RM, Shah RB, Smith SC, Tickoo S, Tretiakova MS, True L, Verkarre V, Wobker SE, Zhou M, Gill AJ (2021) New developments in existing WHO entities and evolving molecular concepts: the genitourinary pathology society (GUPS) update on renal neoplasia. Mod Pathol 34:1392–1424. https://doi.org/10.1038/s41379-021-00779-w
67. Cipriani NA, Agarwal S, Dias-Santagata D, Faquin WC, Sadow PM (2017) Clear cell change in thyroid carcinoma: a clinicopathologic and molecular study with identification of variable genetic anomalies. Thyroid 27:819–824. https://doi.org/10.1089/thy.2016.0631
68. Val-Bernal JF, Martino M (2020) Clear cell change in follicular adenoma of the thyroid. A diagnostic challenge. Rom J Morphol Embryol 61:219–226. https://doi.org/10.47162/RJME.61.1.24
69. Zur KB, Brandwein M, Wang B, Som P, Gordon R, Urken ML (2002) Primary description of a new entity, renal cell-like carcinoma of the nasal cavity: van Meegeren in the house of Vermeer. Arch Otolaryngol Head Neck Surg 128:441–447. https://doi.org/10.1001/archotol.128.4.441
70. Bernstein JM, Montgomery WW, Balogh K (1966) Metastatic tumors to the maxilla, nose, and paranasal sinuses. Laryngoscope 76:621–650. https://doi.org/10.1288/00005537-196604000-00003
71. Bastier P-L, Dunion D, de Bonnecaze G, Serrano E, de Gabory L (2018) Renal cell carcinoma metastatic to the sinonasal cavity: a review and report of 8 cases. Ear Nose Throat J 97:E6–E12. https://doi.org/10.1177/014556131809700902
72. Storck K, Hadi UM, Simpson R, Ramer M, Brandwein-Gensler M (2008) Sinonasal renal cell-like adenocarcinoma: a report on four patients. Head Neck Pathol 2:75–80. https://doi.org/10.1007/s12105-008-0047-4
73. Shen T, Shi Q, Velosa C, Bai S, Thompson L, Simpson R, Wei S, Brandwein-Gensler M (2015) Sinonasal renal cell-like adenocarcinomas: robust carbonic anhydrase expression. Hum Pathol 46:1598–1606. https://doi.org/10.1016/j.humpath.2015.06.017
74. Yuan CC, Zhai CW, Wang SY (2020) Sinonasal renal cell-like adenocarcinoma: a clinicopathological analysis of five cases. Zhonghua Bing Li Xue Za Zhi 49:1147–1151. https://doi.org/10.3760/cma.j.cn112151-20200206-00070

75. Wasserman JK, Gravel D, Purgina B (2018) Chordoma of the head and neck: a review. Head Neck Pathol 12:261–268. https://doi.org/10.1007/s12105-017-0860-8
76. Yadav R, Sharma MC, Malgulwar PB, Pathak P, Sigamani E, Suri V, Sarkar C, Kumar A, Singh M, Sharma BS, Garg A, Bakhshi S, Faruq M (2014) Prognostic value of MIB-1, p53, epidermal growth factor receptor, and INI1 in childhood chordomas. Neuro Oncol 16:372–381. https://doi.org/10.1093/neuonc/not228
77. Shih AR, Cote GM, Chebib I, Choy E, DeLaney T, Deshpande V, Hornicek FJ, Miao R, Schwab JH, Nielsen GP, Chen Y-L (2018) Clinicopathologic characteristics of poorly differentiated chordoma. Mod Pathol 31:1237–1245. https://doi.org/10.1038/s41379-018-0002-1
78. Hoch BL, Nielsen GP, Liebsch NJ, Rosenberg AE (2006) Base of skull chordomas in children and adolescents: a clinicopathologic study of 73 cases. Am J Surg Pathol 30:811–818. https://doi.org/10.1097/01.pas.0000209828.39477.ab
79. Thompson LDR (2011) Chordoma. Ear Nose Throat J 90:16–18. https://doi.org/10.1177/014556131109000105
80. Merna C, Lehrich BM, Kshirsagar RS, Eide JG, Diaz-Aguilar LD, Goshtasbi K, Yasaka TM, Sahyouni R, Palmer JN, Adappa ND, Hsu FPK, Kuan EC (2022) Determinants of survival in skull base chondrosarcoma: a national cancer database study. World Neurosurg 158:e766–e777. https://doi.org/10.1016/j.wneu.2021.11.066
81. Antonescu CR, Zhang L, Chang N-E, Pawel BR, Travis W, Katabi N, Edelman M, Rosenberg AE, Nielsen GP, Dal Cin P, Fletcher CDM (2010) EWSR1-POU5F1 fusion in soft tissue myoepithelial tumors. A molecular analysis of sixty-six cases, including soft tissue, bone, and visceral lesions, showing common involvement of the EWSR1 gene. Genes Chromosomes Cancer 49:1114–1124. https://doi.org/10.1002/gcc.20819
82. Modi S, Goel D, Goyal P, Gupta A (2020) Primary myoepithelial carcinoma of the clivus: a rare presentation. Asian J Neurosurg 15:1024–1026. https://doi.org/10.4103/ajns.AJNS_144_20
83. Soo MYS, Ng T, Gomes L, da Cruz M, Dexter M (2004) Skull base chordoid meningioma: imaging features and pathology. Australas Radiol 48:233–236. https://doi.org/10.1111/j.1440-1673.2004.01278.x
84. Umphress B, Raparia K (2018) Rhinoscleroma. Arch Pathol Lab Med 142:1533–1536. https://doi.org/10.5858/arpa.2018-0073-RA
85. Elwany S, Fattah HA, Mandour Z, Ismail AS, Abdelnabi M (2020) A myriad of scleroma presentations: the usual and unusual. Head Neck Pathol 14:588–592. https://doi.org/10.1007/s12105-019-01075-5
86. Chou T-C, Tsai K-B, Lee C-H (2013) Emperipolesis is not pathognomonic for Rosai-Dorfman disease: rhinoscleroma mimicking Rosai-Dorfman disease, a clinical series. J Am Acad Dermatol 69:1066–1067. https://doi.org/10.1016/j.jaad.2013.08.036